The 11th
International Conference on
Materials and Metallurgical Engineering
November 15, 2022, Tehran

iMat 2022

یازدهمین کنفرانس بین المللی مهندسی مواد و متالورژی ایران
شانزدهمین کنفرانس مشترک انجمن مهندسین متالورژی و انجمن ریخته گری ایران
بیست و ششمین کنگره سالانه انجمن مهندسین متالورژی ایران
۲۴ آبان ماه ۱۴۰۱/ تهران

The effect of annealing treatment on thermoelectric properties of nanostructured $Bi_{0.5}Sb_{1.5}Te_3$ thin films fabricated by Hydrothermal method and thermal evaporation

Davood Zahiri Rad[1],Hamta Mansouri[2], Seyed Abdolkarim Sajjadi[3],Yasaman Saberi Kakhki [4]

Hamta.mansouri@gmail.com

Abstract

Bismuth antimony telluride ($Bi_{0.5}Sb_{1.5}Te_3$) is one of the best-known thermoelectric compounds. The powder of $Bi_{0.5}Sb_{1.5}Te_3$ was hydrothermally synthesized for 24 hours at 150°C. Thermal evaporation was used to deposit $Bi_{0.5}Sb_{1.5}Te_3$ thin films. Subsequently, annealing treatment was performed on one of the thin films at 373 K for 1 h. X-ray diffraction (XRD) and field emission scanning electron microscopy (FESEM) and PSA (particle size analysis) were used to investigate powders and thin films. The phase and microstructure results of the synthesized powders showed that $Bi_{0.5}Sb_{1.5}Te_3$ powder was formed. Thermoelectric results demonstrated that annealing of thin films causes increasing of the Seebeck coefficient from195 to 373 µV/K at 323 K. However, the power factor of the annealed thin films was measured as $0.06*10^{-6}$ µW/k^2.cm in comparison to that of the unannealed thin films which was measured as $0.1*10^{-6}$ µW/k^2.cm at 323 K.

Keywords*:* Thermoelectric material; thin film; bismuth antimony telluride; annealing; Seebeck coefficient; nanostructure.

1- Introduction

Thermoelectric materials (TE) are semiconductors converting electricity to heat without any moving parts, noise, or pollution [1,2]. Global environmental concerns can cause Researchers interest to investigate thermoelectric devices as new technologies [3]. The performance of TE materials (PF) is deliberated by a power factor parameter based on equation (1):

$$PF=S^2\delta \quad (1)$$

in which, S is the Seebeck coefficient and δ is the electrical conductivity [3]. The amount of power factor can be evaluated as the capability of the thermal to electrical energy conversion.

[1] - M. Sc Student, Department of Materials Science and Engineering, Faculty of Engineering, Ferdowsi University of Mashhad, Mashhad, Iran.
[2] – Undergraduate Student, Department of Materials Science and Engineering, Faculty of Engineering, Ferdowsi University of Mashhad, Mashhad, Iran.
[3] – Full Professor, Department of Materials Science and Engineering, Faculty of Engineering, Ferdowsi University of Mashhad, Mashhad, Iran.
[4] – Post Doctorate Researcher, Department of Materials Science and Engineering, Faculty of Engineering, Ferdowsi University of Mashhad, Mashhad, Iran.

The maximum quantity of the figure of merit was about 1.0 [4]. Different methods for the manufacturing of these compounds were used including solvothermal [5], hydrothermal [6], melt spinning [7], microwave synthesis [8], and mechanical alloying (MA), followed by hot pressing or spark plasma sintering (SPS) [9]. The hydrothermal method has significant features like low energy, low cost, and low energy consumption and has direct production at low temperatures [10].

The best-known thermoelectric materials are those based on bismuth telluride [11, 12]. These materials achieved their highest merit at room temperature [13]. As compared with the other thermoelectric materials, group IV–VI compounds have the best electrical transport properties, narrow band gaps, and a higher figure of merit [14, 15].

The annealing process improved some thermoelectric properties. As a result of these improvements, the Seebeck coefficient is increasing. During annealing, however, antisite defects decreased the electrical conductivity. Annealing can have a significant impact on the Seebeck coefficient and electrical conductivity.

2- Experimental

To synthesize $Bi_{0.5}Sb_{1.5}Te_3$ by hydrothermal method, Te powders (0.957 g), $BiCl_3$ (0.39 g), $SbCl_3$ (0.855 g), EDTA (0.16 g), $NaBH_4$ (0.370 g), and NaOH (0.27 g) were used. The raw materials were obtained from Sigma Aldrich (Germany).

At first, EDTA (0.16 g) was added to a solvent (a ratio of Ethanol to water was 8:1) and stirred for 10 min. Afterward, 0.957 g Te, 0.37 g $NaBH_4$, 0.27 g NaOH (as an agent to control pH) and $BiCl_3$ (0.39 g), $SbCl_3$ (0.855 g) were added step by step into the solution and stirred again for 10 min. All the procedures were performed in an N_2 atmosphere in a glove box. Finally, the obtained solution was transferred into a Teflon-lined stainless-steel autoclave up to 80% of its capacity. The container with the solution was kept in a furnace at 150 °C for 24 h and then it was cooled gradually in the furnace.

Finally, the black liquid obtained from the synthesis procedure was washed three times using distilled water and acetone and finally was dried under a vacuum at 100 °C for 6 h. XRD analysis of the synthesized powders was carried out by a AW-XDM300 diffractometer using Cu-Kα radiation (λ=0.154) in the 2-theta range 20-70°. The particle size of the synthesized powders was measured using a particle size analyzer (Vasco3-Cordoun).

$Bi_{0.5}Sb_{1.5}Te_3$ thin films were produced by a deposition procedure using the thermal evaporation method (EDS-160/Iran) with a current of 70 A. The thermal evaporation method was employed in a high-vacuum chamber under a pressure of about 1.33×10^{-7} kPa and with a deposition rate of 5 A°/S. In this work, the thermoelectric thin films deposited at the substrate temperature of 100 °C were selected and the work was continued in two conditions: without annealing

treatment and with annealing treatment at 373K for 1h. Two thin films with a thickness of 90.11 nm were prepared under chamber pressure of about 10^{-6} torr. Microstructural study of the produced compounds and thin films was carried out by scanning electron microscopy (FESEM, TESCAN MIRA 30XMU) using an accelerating voltage of 10 kV with a secondary electron detector. The chemical composition of different phases that existed in the samples was determined by energy-dispersive X-ray spectra (EDS). Ultraviolet-Visible (UV–Vis) spectra were investigated in the wavelength range from 190 nm to 1100 nm by Lambod UVD2950 UV spectrometer. The Seebeck coefficient (α) was measured using the SRM1/Iran instrument. Finally, the electrical conductivity (δ), carrier concentration, and mobility were measured using a Hall measurement system (Ecopia/Korea).

3- Results and Discussion

3.1. Phase analysis

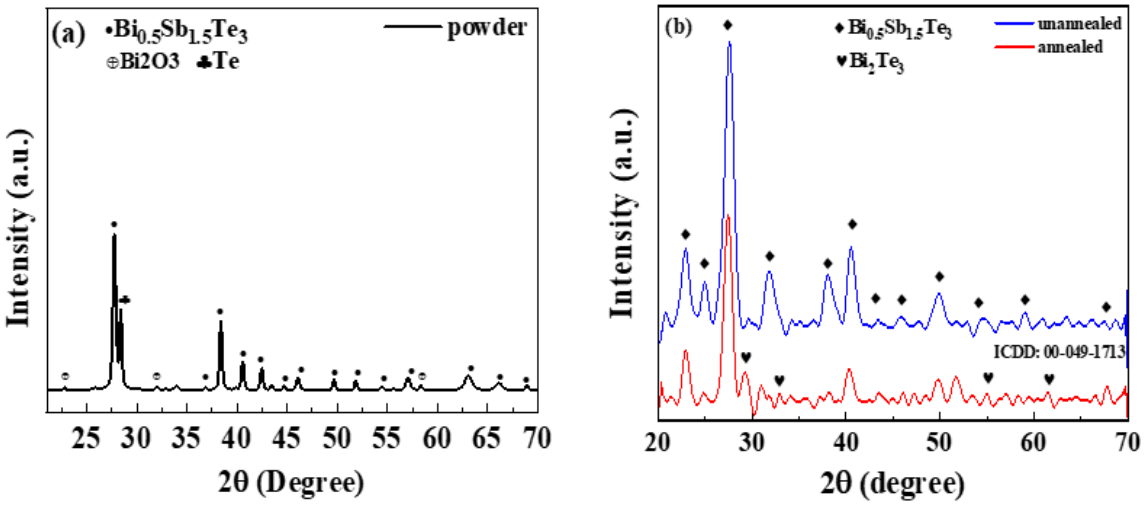

Figure 1: XRD patterns of (a) hydrothermally synthesized $Bi_{0.5}Sb_{1.5}Te_3$ powder and (b) annealed and unannealed $Bi_{0.5}Sb_{1.5}Te_3$ thin films.

Figure 1(a) shows X-ray diffraction patterns of the $Bi_{0.5}Sb_{1.5}Te_3$ powders synthesized by hydrothermal procedure at 150 °C. It is found that the $Bi_{0.5}Sb_{1.5}Te_3$ ternary compound (JPDS No.721835) is formed however, some impurities can be detected [16]. Te segregation could be related to the van der walls bonding in Bi_2Te_3 based [17].

Figure 1(b) shows XRD patterns of the unannealed and annealed thin films. Both films are polycrystalline and have rhombohedral structures and prominent peaks at (015, 1010, and 0111) [18,19]. The peak intensities decreased with annealing treatment [20]. It shows that the intensity of the main peaks of $Bi_{0.5}Sb_{1.5}Te_3$ thin films are influenced by annealing treatment that the

crystallinity of the thin films is decreased by annealing and also it can be seen that the other binary phase like Bi_2Te_3 was existed which may cause an important effect on thermoelectric properties.

3.2. Microstructural analysis

FESEM images of $Bi_{0.5}Sb_{1.5}Te_3$ synthesized powders produced at 150 °C are given in Figure 2 (a,b) due to this figure, the powder presents a regular morphology with a plate-like structure and a thickness of 17.31 nm, which was measured by Digimizer software. The plate-like morphology of the hydrothermal powders was reported by Dharmaiah et al. [16]. Figure 2 (c) presents the chemical composition of hydrothermal powders gained by EDS analysis. Obviously, the excellent Bi:Sb:Te stoichiometric composition confirms the successful fabrication process of $Bi_{0.5}Sb_{1.5}Te_3$ powder. EDS results show that synthesized by the hydrothermal method is 66.25:21.19:12.55. the powder morphology and size can be influenced by some parameters like process time, temperature, and type of chemical composition. the average particle size distribution of powders exhibited 73.38 nm. moreover, the uniform size distribution of the fabricated coarse powder and the homogeneity of grains are observed.

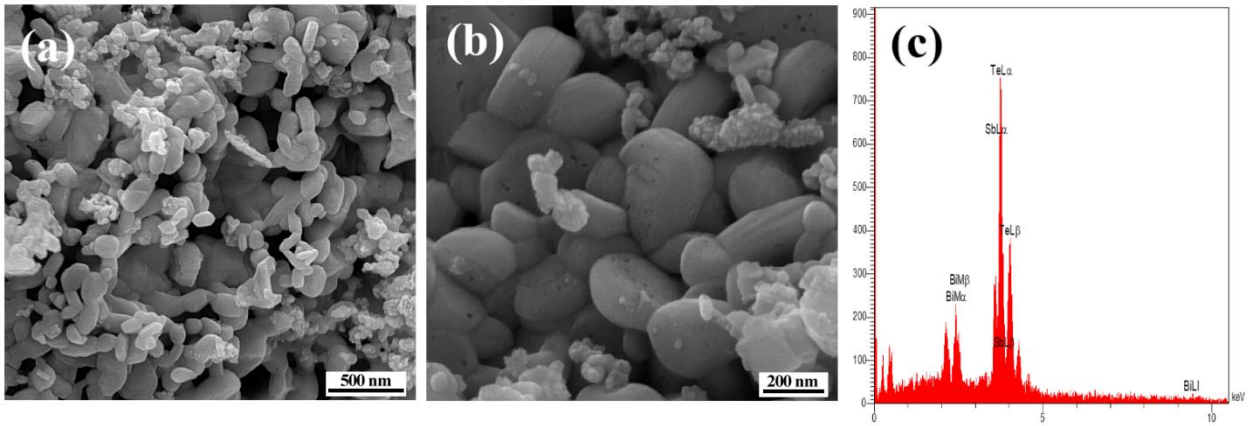

Figure 2: (a,b) FESEM micrographs of $Bi_{0.5}Sb_{1.5}Te_3$ powder prepared by hydrothermal process at different magnifications and (c) the relevant EDS spectrum of the $Bi_{0.5}Sb_{1.5}Te_3$ powder.

FESEM images were used to study the morphological properties of thin films after annealing. Fig. 3 presents microstructures of the unannealed and annealed nano-structured thin films at different magnifications. Unannealed grains have a spherical shape and their grain boundaries are wider than those of annealed grains. As a result of the diffusion of Te in Bi and the more uniform distribution of the elements in the thin films after annealing, narrow gaps may be observed [21]. Unannealed samples have a greater degree of uniformity than annealed samples. Additionally, FESEM images show that grain size decreases after annealing. It is confirmed by the XRD analysis.

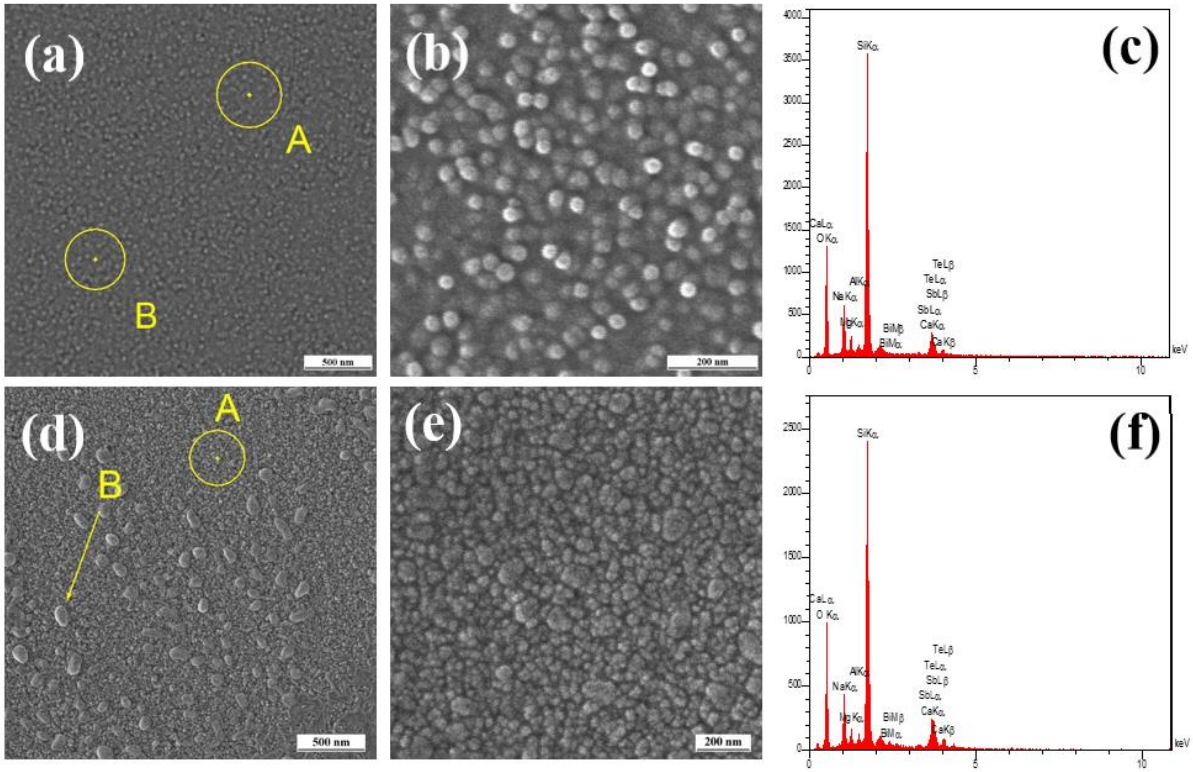

Figure 3: (a,b) FESEM micrographs of annealed $Bi_{0.5}Sb_{1.5}Te_3$ thin film at different magnifications, (c) the relevant EDS spectrum of the annealed $Bi_{0.5}Sb_{1.5}Te_3$ thin film, (d,e) FESEM micrographs of the unannealed thin film at different magnifications and (f) the relevant EDS spectrum of the unannealed $Bi_{0.5}Sb_{1.5}Te_3$ thin film.

Cross-section of the thin film materials (Fig. 4) confirmed that the films have dense structure with thickness of approximately 90.11 nm. Such a dense and crystalline microstructure

produced in Sb_2Te_3/Bi_2Te_3 bilayer thin film reported by Zhang [22]. These properties come from the temperature and time of the hydrothermal process, deposition and annealing parameters.

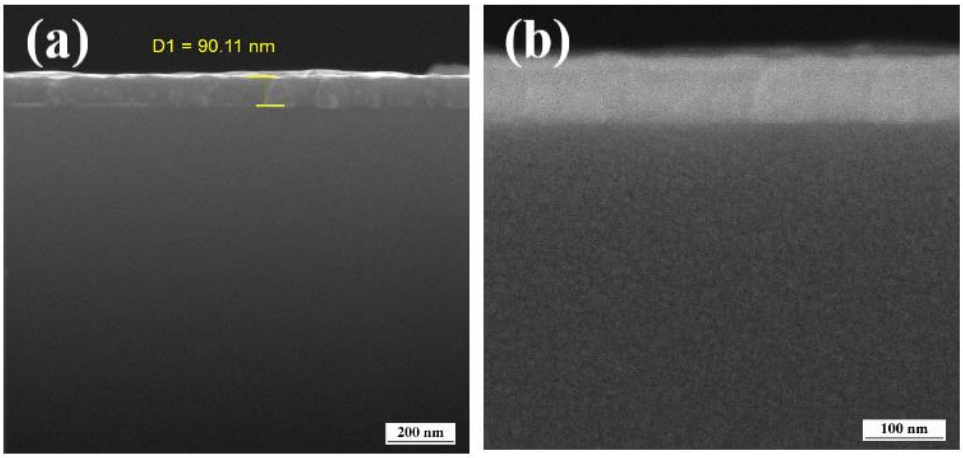

Figure 4 : Cross-sectional FESEM images of unannealed and annealed $Bi_{0.5}Sb_{1.5}Te_3$ thin films at different magnifications.

3.3. Optical Properties

Figure 5 presents the UV-Visible spectra of $Bi_{0.5}Sb_{1.5}Te_3$ samples. It should be mentioned that the band gap energy (Eg) obeys Tauc's equation as follows:

$$\alpha h\nu = A(h\nu - Eg)^n \quad (3)$$

where Eg is the band gap, α is the absorption coefficient, V is the frequency and A is a constant. The value of the "n" could be 1⁄2 or 3⁄2 for direct allowed and 2 or 3 for indirect allowed [23,24,25]. It was found that n=2 offers the best linear graph in the band gap zone. According to Tauc's equation, the amount of band gap energies for the annealed and unannealed samples were 1.16 eV and 1.93 eV, respectively. The higher band gap energy of the annealed sample can be related to its lower crystallinity. Band gap energy is also related to the thickness of thin films. And the higher thicknesses have a lower band gap [26]. Thin films have higher band gap energy compared to the bulk samples due to the nano grain size of the thin films due to an increase in grain size [27].

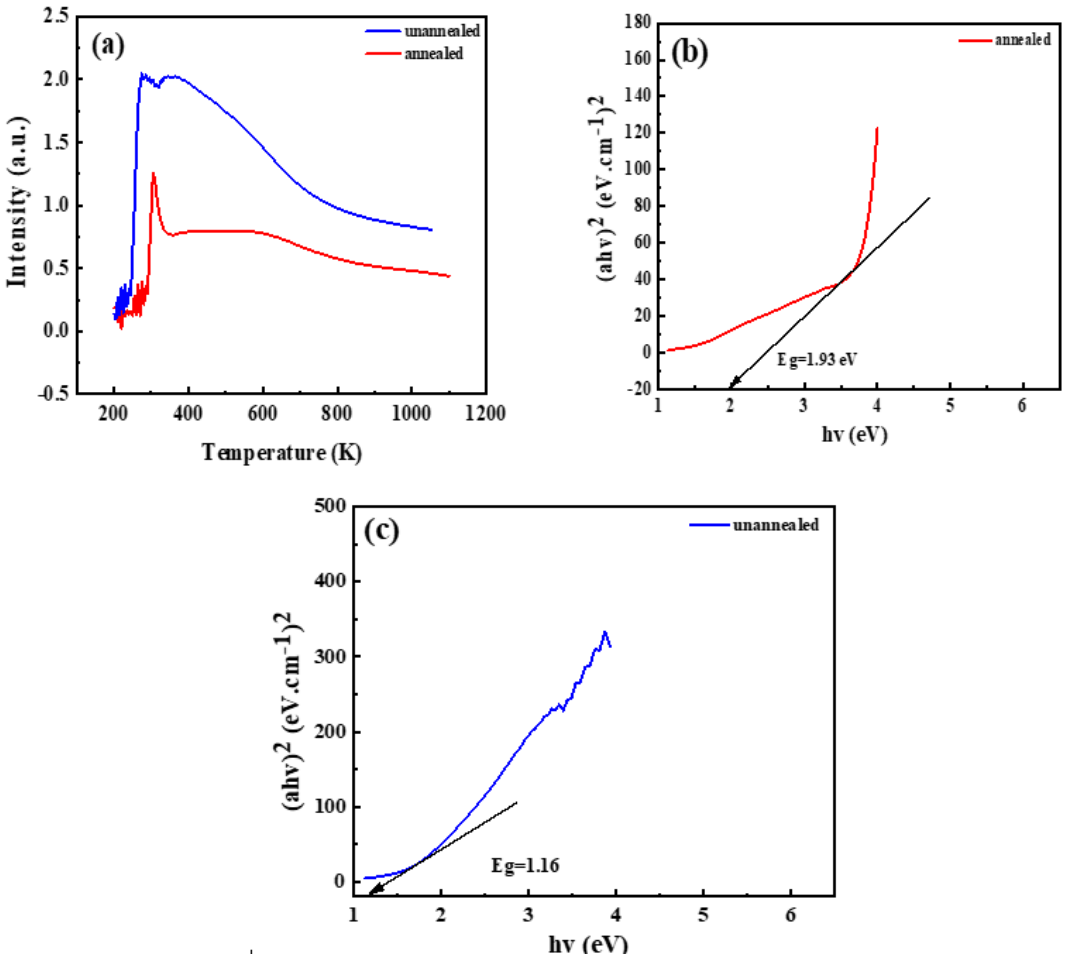

Figure 5 : (a) UV-vis spectra of $Bi_{0.5}Sb_{1.5}Te_3$ thin films prepared by hydrothermal method, (b) plot of $(\alpha h\nu)^2$ as a function of hν for unannealed $Bi_{0.5}Sb_{1.5}Te_3$ thin film, and (c) plot of $(\alpha h\nu)^2$ as a function of hν for annealed $Bi_{0.5}Sb_{1.5}Te_3$ thin film.

3.4. Seebeck Coefficient

Figure 6 exhibits the Seebeck coefficient for both thin films in the temperature range of 323 K to 473 K. Seebeck coefficient values for both samples present the p-type semiconductor behavior according to the positive sign. Furthermore, the Seebeck coefficient of the annealed sample at all temperatures is increasing compared with the unannealed sample.

The enhancing of the Seebeck coefficient in the annealed thin film can show the influence of the annealing on the increase of Sb_{Te} anitisites due to the increase of the hole concentration [28].

the maximum Seebeck coefficient of the annealed sample (571 μV/K) is observed at 473 K and in the case of the unannealed sample (317 μV/K) is observed at 473 K. The values of the Seebeck coefficient at room temperature for the unannealed and annealed samples were 195 and 373 μV/K, respectively. The maximum Seebeck coefficient of the annealed sample (571 μV/K) is observed at 473 K and in the case of the unannealed sample (317 μV/K) is observed at 473 K. The values of the Seebeck coefficient at room temperature for the unannealed and annealed samples were 195 and 373 μV/K, respectively.

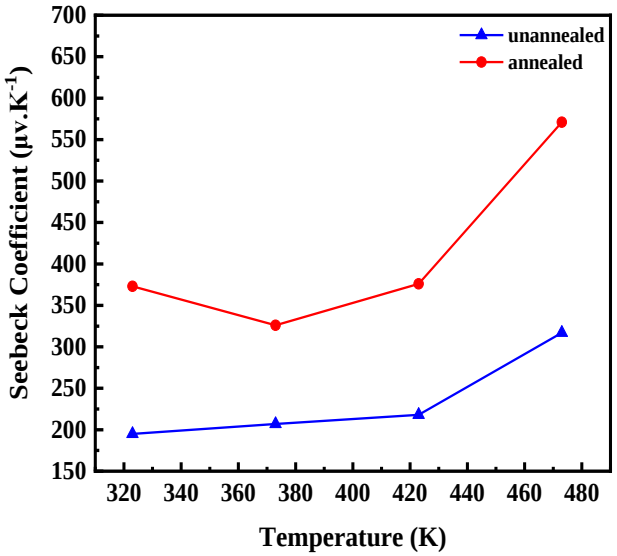

Figure 6 : Temperature dependence of the Seebeck coefficient for the annealed and unannealed $Bi_{0.5}Sb_{1.5}Te_3$ thin films.

3.5. Electrical transport properties

Figure 7(a) demonstrates the Hall measurement results of the annealed and unannealed thin film. the Hall coefficient measurements show a positive sign at room temperature. It confirms that the thin film material is a p-type semiconductor and the carriers in p-type semiconductors are holes [29]. Figure 7(b) shows the effect of annealing treatment on the electrical conductivity. On the right, it can be seen that the nano-grain size of annealed thin film (84 nm) measured by Digimizer software) is smaller than unannealed thin film (90 nm). It means the lower grain size of the annealed thin film led to the reduction of the electrical conductivity. It can be attributed to the effect of the grain boundaries on the reduction of the electrons' movement. Due to the low temperature of the substrate and the lack of a substrate heat treatment, antisites were created during the deposition of annealed samples, resulting in lower electrical conductivity. During

annealing, impurities and different phases like Bi_2Te_3 are also responsible for lower electrical conductivity.

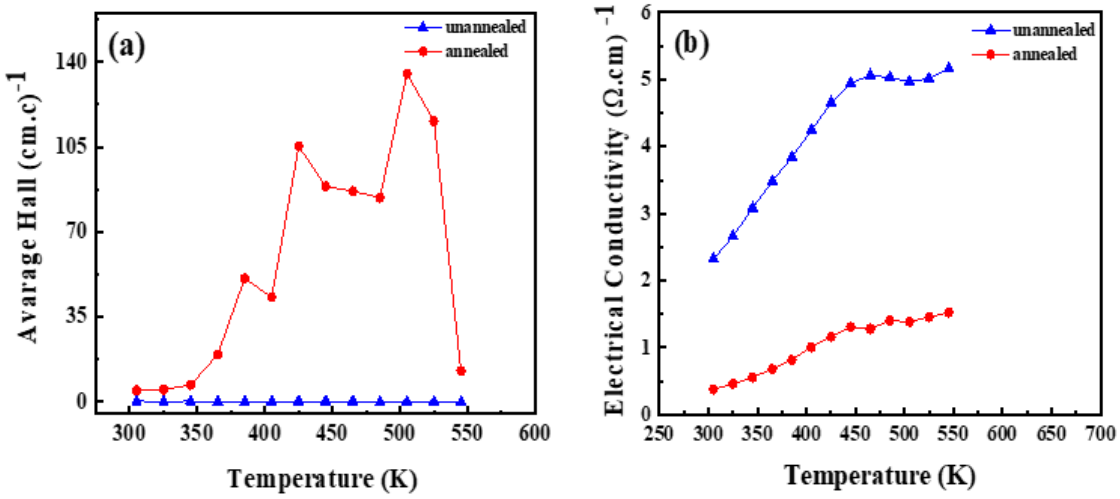

Figure 7: (a) Hall measurement results of the annealed and unannealed thin film, (b) the effect of annealing treatment on the electrical conductivity.

3.6. Power Factor

Figure 8 shows the power factor of the two $Bi_{0.5}Sb_{1.5}Te_3$ thin films. The value demonstrates the efficiency of thermoelectric properties and can be calculated by $PF = \delta\alpha^2$ formula [30]. The power factor of these two thin films (annealed and unannealed) were $0.4*10^{-6}$ and $0.8*10^{-6}$ $\mu W/cm.k^2$, at 473 K, respectively. According to the results, a higher power factor for the annealed sample was achieved in comparison with the unannealed sample. After the annealing treatment, the Seebeck coefficient became higher but electrical conductivity decreased because of the impurities and some antisite defects. The higher crystallinity of the unannealed thin film is the other reason of increase in power factor.

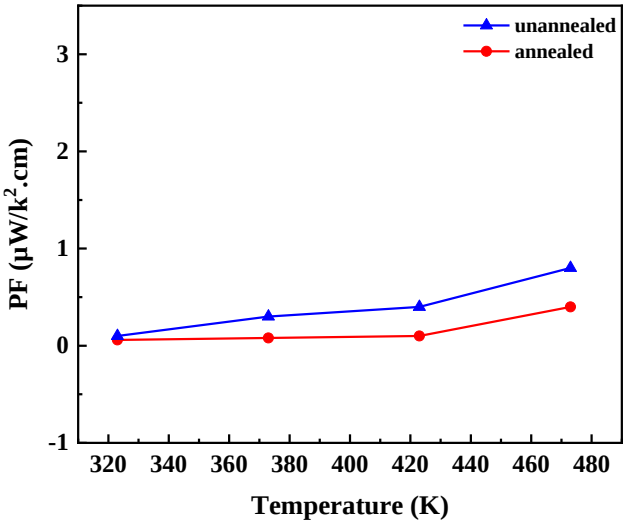

Figure 8: Temperature dependence of the power factor of annealed and unannealed $Bi_{0.5}Sb_{1.5}Te_3$ thin films.

4- Conclusions

We synthesized $Bi_{0.5}Sb_{1.5}Te_3$ thin films by hydrothermal method followed by thermal evaporation. Morphology, particle size, bandgap energy, and thermoelectric properties were characterized. The obtained results were summarized as follows:

1. Seebeck coefficient values for both samples determined the p-type behavior of the semiconductors.
2. The lowest band gap was gained for the unannealed thin film due to the higher crystallinity.
3. Higher power factor for the unannealed sample was achieved in comparison with the annealed sample.
4. Seebeck coefficient values for both samples present the p-type semiconductor behavior.
5. The maximum amount of Seebeck coefficient was achieved for the annealed thin film due to the increase of Sb_{Te} anitisites and so the increase of the hole concentration.

References

[1]El Fatnani FZ, Guyomar D, Mazroui M, "Optimization and improvement of thermal energy harvesting by using pyroelectric materials". Opt Mater (Amst) 56:22–26.

[2]Z. He, Y.X. Chen, Z. Zheng, F. Li, G. Liang, J. Luo, P. Fan. "Enhancement of thermoelectric performance of N-type Bi2Te3 based thin films via in situ annealing during magnetron sputtering", Ceram. Int. 46:13365–13371.

[3]Y. Saberi, S.A. Sajjadi, H. Mansouri (2021), "Comparison of thermoelectric properties of Bi2Te3 and Bi2Se0·3Te2.7 thin film materials synthesized by hydrothermal process and thermal evaporation", Ceram. Int. 47:11547–11559.

[4]Z. Ma, J. Wei, P. Song, M. Zhang, L. Yang, J. Ma, W. Liu, F. Yang, X. Wang, " Review of experimental approaches for improving zT of thermoelectric materials", Mater. Sci. Semicond. Process. 121 - 105303.

[5] W. Wang, B. Poudel, J. Yang, D.Z. Wang, Z.F. Ren, "High yield synthesis of single-crystalline antimony telluride hexagonal nanoplates using a solvothermal approach". J Am Chem Soc 127, 13792–13793.

[6] P. Dharmaiah, S.J. Hong, "Hydrothermal method for the synthesis of Sb2Te3, and Bi0.5Sb1.5Te3 nanoplates and their thermoelectric properties". Int. J. Appiedl. Ceramic. Technology. 15, 132–139.

[7] S. Fan, J. Zhao, J. Guo, Q. Yan, J. Ma, H.H. Hng, " P-type Bi0.4Sb1.6Te3 nanocomposites with enhanced figure of merit". Appl. Physics. Letter. 96, 2010–2013.

[8]A. Kadhim, A. Hmood, H.A. Hassan, "Physical properties of Bi2(Te, Se)3and Bi2Se1.2Te1.8 prepared sing solid-state microwave synthesis". Materials. Letter. 65, 3105–3108 (2011).
[9] B. Poudel, Q. Hao, Y. Ma, Y. Lan, A. Minnich, B. Yu, X. Yan, D. Wang, A. Muto, D. Vashaee, X. Chen, J. Liu, M.S. Dresselhaus, G. Chen, Z. Ren, "High-thermoelectric performance of nanostructured bismuth antimony telluride bulk alloys". J. Science.

[10] Suvacı, Ender, and Emel Özel. "Hydrothermal synthesis." Encyclopedia of Materials: Technical Ceramics and Glasses. ISBN: 9780128222331.

[11] S. Bano, A. Kumar, B. Govind, A.H. Khan, A. Ashok, D.K. Misra, Room temperature Bi2Te3-based thermoelectric materials with high performance. J. Mater. Sci. Mater. Electron. 31, 8607–8617.

[12] P. Dharmaiah, H. Kim, C. Lee, S. Hong, "Influence of powder size on thermoelectric properties of p-type 25%Bi2Te3-75%Sb2Te3 alloys fabricated using gas atomization and spark-plasma sintering". J.Alloys&Compd.

[13] H. Zhang, F. Ye, Y. Hu, J. Liu, Y. Zhang, Y. Wu, Z. Hu, "The investigation of thermal properties

on multilayer Sb2Te3/Au thermoelectric material system with ultra-thin Au interlayers". Superlattices Microstruct. 89, 312–318.

[14] Shafique, Aamir, and Young-Han Shin. "Thermoelectric and phonon transport properties of two dimensional IV–VI compounds" Scientific reports 7, no. 1 :1-10.

[15]11. Y. Dou, X. Yan, Y. Du, J. Xu, D. Li, " Thermoelectric properties of Bi0.4Sb1.6Te3-based composites with silicon nano inclusions". J. Mater. Sci. Mater. Electron. 31, 4808–4814.

[16] Dharmaiah, Peyala, and Soon-Jik Hong. "Hydrothermal method for the synthesis of Sb2Te3, and Bi0. 5Sb1. 5Te3 nanoplates and their thermoelectric properties." International Journal of Applied Ceramic Technology 15, no. 1: 132-139.

[17] Witting, Ian T., Thomas C. Chasapis, Francesco Ricci, Matthew Peters, Nicholas A. Heinz, Geoffroy Hautier, and G. Jeffrey Snyder. "The thermoelectric properties of bismuth telluride." Advanced Electronic Materials 5, no. 6: 1800904.

[18]S. Kianwimol, R. Sakdanuphab, N. Chanlek, A. Harnwunggmoung, A. Sakulkalavek , Surf. Coatings Technol. 393:125808.

[19]H. Mansouri, S.A. Sajjadi, A. Babakhani, Y. Saberi (2021), J. Mater. Sci. Mater. Electron. 32:9858–9871.

[20]Wang, Hong Jun, and Yuan Yuan Zhu. "Effect of post-annealing on the structure and optical properties of ZnO films deposited on Si substrates." In IOP Conference Series: Materials Science and Engineering, vol. 382, no. 2, p. 022054.

[21]Arora, Swati, Vivek Jaimini, Subodh Srivastava, and Y. K. Vijay. "Properties of nanostructure bismuth telluride thin films using thermal evaporation." Journal of Nanotechnology.

[22] Zheng, Zhuang-hao, Ping Fan, Jing-ting Luo, Xing-min Cai, Guang-xing Liang, Dong-ping Zhang, and Fan Ye. "Thermoelectric properties of bismuth antimony tellurium thin films through bilayer annealing prepared by ion beam sputtering deposition." Thin Solid Films 562 : 181-184.

[23] D. Bourgault, B. Schaechner, C. Giroud Garampon, T. Crozes, N. Caillault, and J. Carbone, Alloys Compd.

[24] Kim, Il-Ho. "Electronic transport properties of the flash-evaporated p-type Bi0. 5Sb1. 5Te3 thermoelectric thin films." Materials Letters 44, no. 2: 75-79.

[25] Mansouri, Hamta, Yasaman Saberi, and Seyed Abdolkarim Sajjadi. "Effect of Hydrothermal Synthesis Temperature on the Microstructural and Thermoelectric Characteristics of Thermally Deposited Bi0. 5Sb1. 5Te3 Thin Films." Journal of Electronic Materials 51, no. 2 :495-507.

[26] C.F. Desai, N.C. Chourasia, S.N. Dhar. "Effect of heat treatment on the optical absorption of BiSbTe3 thin films". J. Materials Letters, 45(2), 116-119.

[27] J. Dheepa, R. Sathyamoorthy, S. Velumani , "Structural and optical investigation of Te-based chalcogenide thin films",Materials. Charact. 58:782–785.

[28] Saberi, Yasaman, Seyed Abdolkarim Sajjadi, and Hamta Mansouri. "Comparison of thermoelectric properties of Bi2Te3 and Bi2Se0· 3Te2. 7 thin film materials synthesized by hydrothermal process and thermal evaporation."J. Ceramics International 47, no. 8 (2021): 11547-11559.

[29] Moumen, Abderrahim, Gayan CW Kumarage, and Elisabetta Comini. "P-Type Metal Oxide Semiconductor Thin Films: Synthesis and Chemical Sensor Applications." Sensors 22, no. 4: 1359.

[30] Saberi, Yasaman, and Seyed Abdolkarim Sajjadi. "A comprehensive review on the effects of doping process on the thermoelectric properties of Bi2Te3 based alloys." J. Alloys and Compounds 163918.